Aerodynamics of a bus with open windows

M.M. Yelmule and S.R. Kale*

Department of Mechanical Engineering,
Indian Institute of Technology Delhi,
New Delhi 110 016, India
Fax: +91 11 2658 2053
E-mail: mukesh.yelmule@ge.com
E-mail: srk@mech.iitd.ac.in
*Corresponding author

S.V. Veeravalli

Department of Applied Mechanics,
Indian Institute of Technology Delhi,
New Delhi 110 016, India
Fax: +91 11 2658 1119
E-mail: svrvalli@am.iitd.ernet.in

Abstract: Most passenger trips worldwide are in open window buses where airflow due to motion provides comfort. The aerodynamics of such a bus was studied. Flow visualisations in a water channel using a 1:25 model showed highly turbulent inflow and outflow through rear and front windows, respectively. Large Eddy Simulation (LES) at the full-scale Reynolds number confirmed these features. Seven different interventions (in the form of slots on different surfaces) were considered. It was found that for the best configuration, the drag was reduced by 29% and the comfort zone increased from 11% to 52% of the passenger volume.

Keywords: bus; open windows; aerodynamics; air circulation; intervention; drag; comfort level.

Reference to this paper should be made as follows: Yelmule, M.M., Kale, S.R. and Veeravalli, S.V. (2009) 'Aerodynamics of a bus with open windows', *Int. J. Heavy Vehicle Systems*, Vol. 16, No. 4, pp.459–488.

Biographical notes: Mukesh M. Yelmule received his BE Degree in the Department of Mechanical Engineering from University of Pune, India in 2002 and MTech Degree in Thermal Engineering from the Department of Mechanical Engineering, Indian Institute of Technology Delhi in 2006. He is currently with GE India Technology Center, Bangalore. His research interests include fluid mechanics and CFD.

S.R. Kale received his BTech Degree in Mechanical Engineering from the Indian Institute of Technology Delhi, India in 1977, and MS and PhD Degrees in Mechanical Engineering from Stanford University, CA in 1981 and 1984, respectively. He has been with the Department of Mechanical

Engineering since 1989 where he is currently Professor. His research interests include energy conversion, sustainable transport and multiphase flows.

S.V. Veeravalli received his BTech Degree in Mechanical Engineering from the Indian Institute of Technology Bombay, India in 1983, and PhD Degree in Mechanical Engineering from Cornell University, NY, in 1989. He was a post-doctoral fellow at the Center for Turbulence Research, Stanford University, CA from 1989 to 1991. Currently, he is Professor in the Department of Applied Mechanics where he has served from 1991. His research interests include stability and turbulence (experiments and modelling).

1 Introduction

Worldwide, buses are the principal means of commuting within and between cities, and for cost reasons, only a small fraction ($<5\%$) of inter-city vehicles are air-conditioned. A vast majority of buses have open windows (as well as doors in some cases) and rely on the motion-induced air circulation for ventilation. Passenger feedback indicates that this arrangement does not provide comfort. Such buses are, however, more eco-friendly as they do not utilise energy for powering an on-board air conditioner. The picture of a typical urban intra-city bus is shown in Figure 1. In a long-term policy perspective of sustainable transport such buses form an important mode that needs to be strengthened. Besides improving fuel economy, passenger comfort is, therefore, a major issue with such buses especially in tropical climates. The aerodynamics of road vehicles has been extensively studied with the objective of drag reduction and, hence, fuel economy improvement. The vehicle has always been modelled as a closed surface with smooth exteriors. The aerodynamics of a vehicle with open windows has not been studied. This study focused first on developing an understanding of the airflow for a bus with open windows and, then, on the effects of design changes on drag and passenger comfort.

In closed vehicles, except for flow through the air-conditioner, there is no fluid connection between the vehicle interior and the surrounding environment. With windows open and in the absence of forced circulation (e.g., by a blower or fan) the flow becomes complex because of the through flow. Traditionally, numerical simulations and wind tunnel tests have been the main techniques for studying such flows and Krajnovic and Davidson (2002) have summarised the state-of-the-art for heavy vehicles, including buses. The Reynolds Averaged Navier-Stokes (RANS) equations have difficulty in predicting momentum transport after separation, which is widely prevalent on a bluff body. The problem is further complicated due to the presence of open windows. Large Eddy Simulation (LES) is better suited but LES of the flow around the full-scale vehicle at the road conditions is difficult because of the fine spatial and time resolution required (Sagaut, 2001). This aspect becomes more acute when windows are open and, consequently, the computation becomes resource intensive. For a bus cruising at 40 km/h, the Reynolds number

based on a typical bus width of 2.5 m is 1.73×10^6. Such Reynolds numbers are difficult to attain in wind tunnels and scaling to lower Reynolds numbers is routinely resorted to (Duell and George, 1999). Complementing wind tunnel and CFD studies is full-scale on-road testing (cf. Mousley and Watkins, 2000). Studies specifically on buses and trucks, for instance Kim (2004), Krajnovic and Davidson (2002) and Roy and Srinivasan (2000), have considered the vehicle body as a closed shape and their objective was aerodynamic drag reduction.

Figure 1 Picture of a typical open-window bus (see online version for colours)

In this study, a complementary combination of visualisation in a water channel at lower Reynolds numbers and numerical simulations at actual Reynolds numbers was adopted. To make the studies well controlled, various simplifications are made. All windows are taken as half-open; in an actual bus, some windows could be fully closed or open, or partially open. The bus compartment is modelled as an empty rectangular box; in actual buses, it is furnished with seats, partitions, and luggage racks, as well as passengers. The doors are closed; in reality doors are often left open. The effect of wheels is not considered. Disturbances due to wind, roadside structures and passing vehicles are not considered – the bus is considered to be moving in an unbounded uniform medium. Passenger compartment dimensions were adopted from those specified for Delhi, 11.6 m long, 2.5 m wide and 2.5 m high. There are eight windows on the right side, winr1–winr8, (driver's side in India) and six on the left side, winl1–winl6. Each window opening is 0.69 m wide and 0.75 m high, and window top edge is 0.375 m below the roof. The windows are not symmetrically located and the distance of the centre of each window from the bus front is given in Table 1.

Table 1 Location of windows in longitudinal direction

Window identifier	*winr1*	*winr2, winl1*	*winr3, winl2*	*winr4, winl3*	*winr5, winl4*	*winr6, winl5*	*winr7*	*winr8, winl6*
Distance bus from front to centroid (m)	0.50	2.03	3.53	5.03	6.53	8.03	8.88	10.40

2 Flow visualisation procedure

Visualisation was performed with a Perspex model with the same external geometry as the actual bus, placed in an open water channel by injecting potassium permanganate solution. The resulting patterns were recorded on still and video cameras. The tip of the needle for introducing the coloured water was positioned with a traverse mechanism at locations depending on the subject feature. The water channel is 0.31 m wide, 0.45 m deep and 12.0 m long. Water flows from an overhead tank and drains into a ground level tank. A steady flow is ensured by maintaining a constant level in the overhead tank and the flow rate was adjusted with a weir plate at channel outlet and an inlet control valve. The model was mounted upright 6 m from the inlet and 30 mm above the channel floor. The size of the model was limited by the permissible blockage which is typically 7.5% of the channel cross-section. The water depth was maintained at 0.42 m, and consequently, the geometrical scale factor was 1 : 25. Figure 2 shows the model that has a brass frame of 6.3 mm square cross-section on which six panels of 4 mm thick Perspex sheet are mounted and joints sealed. Video recordings were performed with a Sony 200X handy cam and frames were extracted from video files.

Figure 2 Picture of the scaled model (see online version for colours)

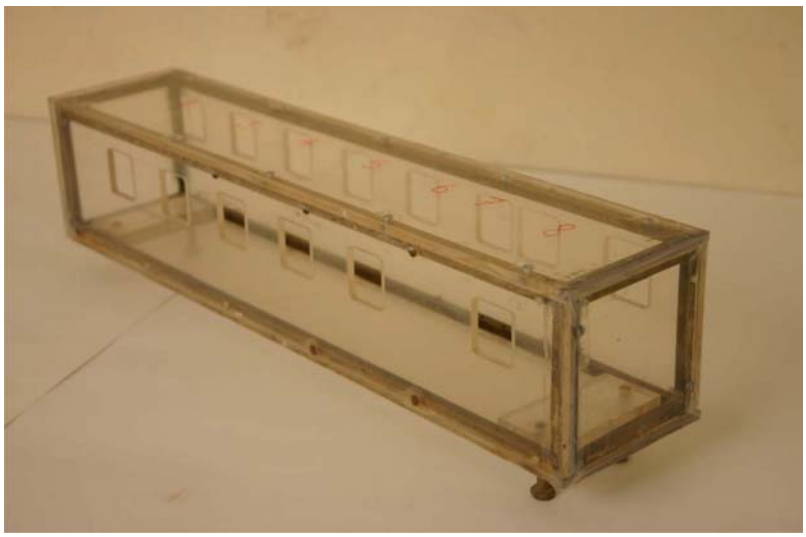

3 Numerical simulations

The flow visualisations showed that both the internal and external flows were highly turbulent with a wide range of length and time scales. Usually, for flow over bluff bodies, there is one characteristic length scale and one characteristic velocity scale, but for semi-closed bodies as in our case, there may be more than one characteristic length scale and velocity scale. The LES method was employed with the RNG-based sub-grid scale model. The filtered conservation equations in Cartesian coordinate system are:

Filtered continuity equation:

$$\frac{\partial \rho}{\partial t} + \frac{\partial}{\partial x_i}(\rho \bar{u}_i) = 0. \tag{1}$$

Filtered momentum equation:

$$\frac{\partial}{\partial t}(\rho \bar{u}_i) + \frac{\partial}{\partial x_j}(\rho \bar{u}_i \bar{u}_j) = \frac{\partial}{\partial x_j}\left(\mu \frac{\partial \bar{u}_i}{\partial x_j}\right) - \frac{\partial \bar{p}}{\partial x_i} - \frac{\partial \tau_{ij}}{\partial x_j}. \tag{2}$$

The sub-grid scale model (Fluent, 2003) is briefly described below. The sub-grid scale stress, τ_{ij}, is defined as:

$$\tau_{ij} = \frac{1}{3}\tau_{kk}\delta_{ij} - 2\mu_t \overline{S}_{ij} \tag{3}$$

where μ_t is the sub-grid scale turbulent viscosity, and $\overline{S}_{ij}$ is the rate-of-strain tensor for the resolved scale defined by

$$\overline{S}_{ij} \equiv \frac{1}{2}\left(\frac{\partial \bar{u}_i}{\partial x_j} + \frac{\partial \bar{u}_j}{\partial x_i}\right). \tag{4}$$

The RNG procedure results in an effective sub-grid viscosity, $\mu_{\text{eff}} = \mu + \mu_t$, given by

$$\mu_{\text{eff}} = \mu[1 + H(x)]^{1/3} \tag{5}$$

where $H(x)$, is the Heaviside function given by

$$H(x) = \begin{cases} x, & x > 0 \\ 0, & x \leq 0 \end{cases}. \tag{6}$$

In the above equation, x is given by

$$x = \frac{\mu_s^2 \mu_{\text{eff}}}{\mu^3} - C \tag{7}$$

where μ_s is given by

$$\mu_s = \rho\left(C_{rng}V^{1/3}\right)^2\sqrt{2\overline{S}_{ij}\overline{S}_{ij}}. \tag{8}$$

Here, V is the volume of the computational cell, and $C_{rng} = 0.157$.

Figure 3 shows the bus model used in the computations. In addition to the windows positioned as per Table 1, the figure shows various intervention slots on the front, rear and top surfaces. As discussed below, several combinations of slot openings were tested.

Figure 3 Nomenclature for windows and interventions

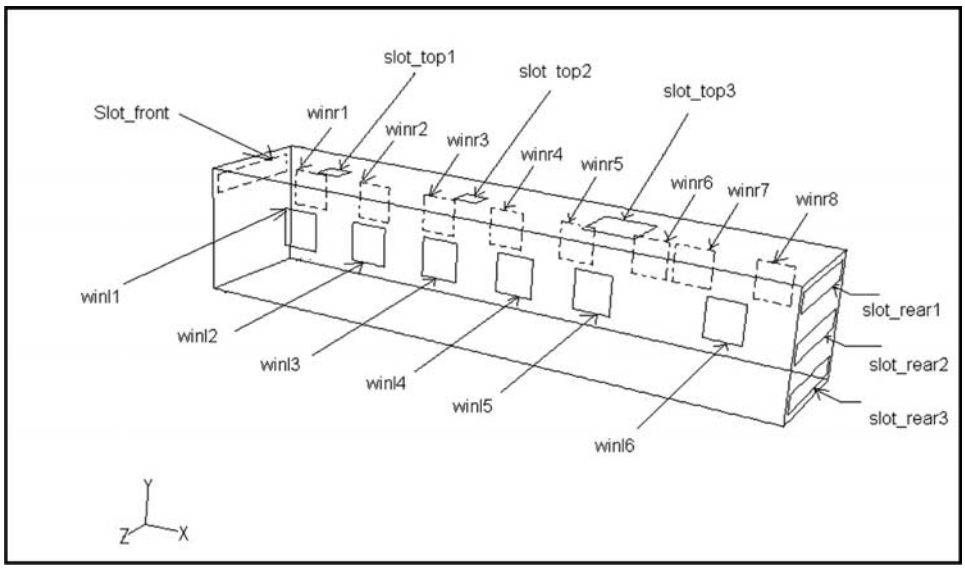

The computations were performed with Fluent® 6.1 on a P-IV 2.8 GHz with 2 GB RAM. The characteristic length in such studies is the width of the vehicle W, which is also the length of largest eddy possible for this flow configuration. The computational domain was 40.6 m (16.24 W) in length, 8 m (3.2 W) wide and 8 m (3.2 W) in height. In the stream-wise direction the model was located 11.6 m (4.64 W) from the inlet and the recovery length downstream of the bus was 17.4 m (6.96 W). In the lateral direction, the bus was placed at domain centre and in the vertical direction the bus floor was 0.4 m (0.16 W) above domain floor. These selections were based on considerations, such as, reduction of the boundary layer effect due to walls, full development of flow, and recovery of velocity and pressure, amongst others. The cells in the interior of the bus are cubical with size of 0.065 m. Outside the bus, the mesh consists of pyramidal cells whose size increases from 0.065 m at bus surface to 0.25 m near the boundary. The total numbers of cells was about 1.89 million. The cell sizes were finalised on the basis of grid independence tests. The equations were solved using the 3-D segregated, implicit, unsteady LES RNG solver while limiting the scaled residuals to 0.001 for continuity and 0.0001 for

velocity components. The convergence was monitored by plotting the drag history over the bus roof. Second order discretisation was used for pressure, whereas for momentum discretisation the second order upwind scheme was used. The unsteady formulation is implicit and second order accurate. The PISO scheme was used for pressure-velocity coupling. The solver was initiated with the vehicle speed ($11.12\,\mathrm{m}\cdot\mathrm{s}^{-1}$) assigned throughout the domain with 5% longitudinal turbulence intensity. The time step was maintained at 0.1 s. We note that the turnover time scale of the smallest resolved eddy is approximately 1 s and, therefore, this choice is conservative. The boundary conditions were

- *at inlet*: velocity ($11.12\,\mathrm{m}\cdot\mathrm{s}^{-1}$ with 5% longitudinal turbulence intensity)
- *at outlet*: pressure (ambient pressure with 5% backflow turbulence intensity)
- *domain walls*: wall moving at vehicle speed
- *walls of bus*: stationary wall
- *interventions (body surfaces)*: interior if open or wall if closed.

Figures 4(a)–(c) show the typical mesh in three planes, vertical normal to the flow (y–z), horizontal (x–z) and vertical longitudinal (x–y), respectively. The convergence specified above has been obtained for each time-step and the computations were continued until fluctuations in drag coefficient dropped to $\pm 7\%$ of the mean value.

Figure 4 The mesh for numerical simulations. Typical views at three planes are shown: (a) a vertical lateral (y–z) plane; (b) vertical longitudinal (x–z) plane and (c) horizontal longitudinal (x–y) plane

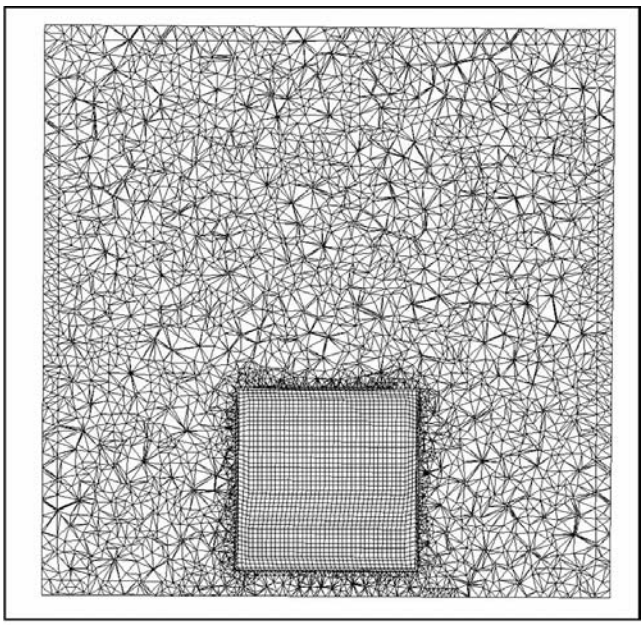

(a)

Figure 4 The mesh for numerical simulations. Typical views at three planes are shown: (a) a vertical lateral (y–z) plane; (b) vertical longitudinal (x–z) plane and (c) horizontal longitudinal (x–y) plane (continued)

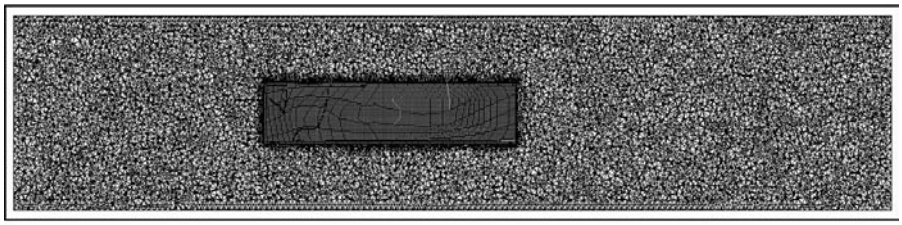

(b)

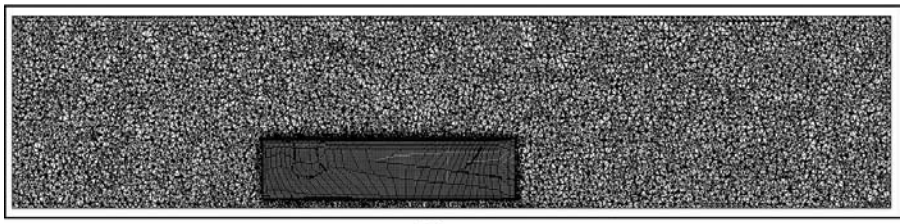

(c)

4 Flow visualisation for reference case (Case 1)

The flow patterns for the reference case, i.e., bus with open windows and no other openings (Case 1) are discussed below. Figures 5–14 are pictures taken with injection at different locations and together reveal the internal and external flows and their interconnections. In all pictures, water flow is from left to right. Two pictures are presented at each window:

- dye injection is inside the model
- injection just outside the window plane, both at window centre.

For clarity, visualisations at the right side windows (winr1 thru winr8) are presented followed by front, roof and wake visualisations.

4.1 Flow at the windows and in the interior

Figure 5(a) shows outflow through the first window (winr1) into the recirculation region that mixes with the free stream. The flow is strongly turbulent and some of the outflow moves towards the roof and into the recirculation region over the roof. Clearly, there is no inflow through this window. Figure 5(b) confirms this feature as water injected outside the window face disperses outwards rapidly. At the second window (winr2), the internal flow is towards the front, and then outwards through winr1 and winl1, Figure 6(a). Figure 6(b) shows some flow towards the front face along the exterior. Together, Figure 5(a) and (b) show a clear outflow through winr1, winr2 and winl1, that mixes into the recirculation region on

the side and partly gets carried out by the free stream. The 3-dimensionality of the turbulent flow causes some upward flow into the recirculation region over the roof. In Figure 7(a), the dye injected inside the bus at the third window (winr3) mixes intensely, moves upstream and exits through winr1, winr2 and winl1. There is no downstream motion. Just outside the window, Figure 7(b), the dye disperses slowly and moves away from the window and there is no strong inflow or outflow through winr3. At the fourth window, winr4, the flow is similar to that at winr3 with flow towards the front face and outwards through all windows ahead of winr4; there is a minor outflow through winr4, Figure 8(a). This pattern is also seen at the opposite left-side window, winl3. Figure 8(b) confirms that there is a slow but clear outflow through winr4. In both these cases, inside flow is wholly towards the front, none towards the rear.

Figure 5 Flow visualisation at the first window on right side (winr1): (a) injection inside the model and (b) injection at the window plane (see online version for colours)

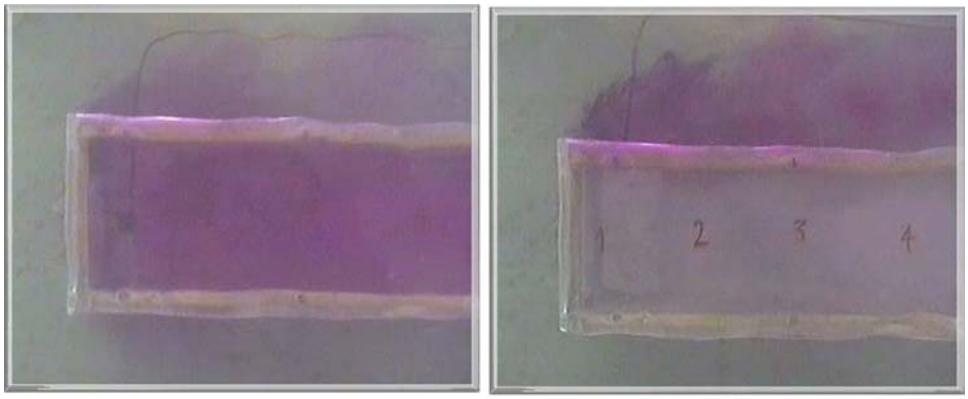

(a) (b)

Figure 6 Flow visualisation at the second window on right side (winr2): (a) injection inside the model and (b) injection at the window plane (see online version for colours)

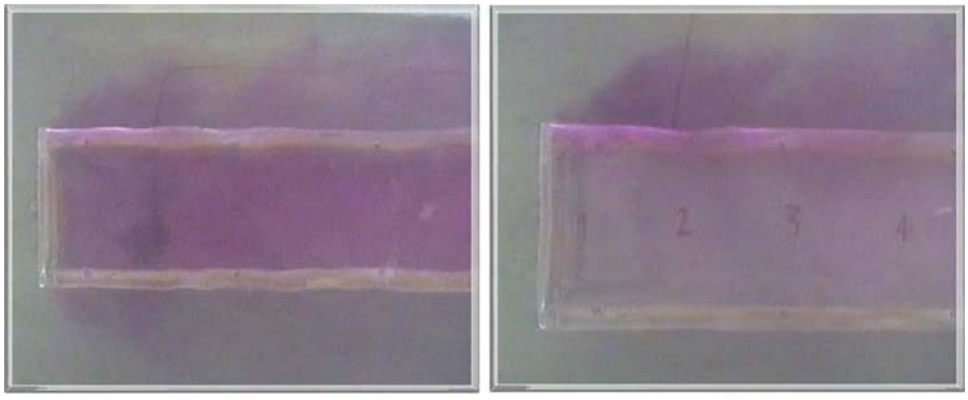

(a) (b)

Figure 7 Flow visualisation at the third window on right side (winr3): (a) injection inside the model and (b) injection at the window plane (see online version for colours)

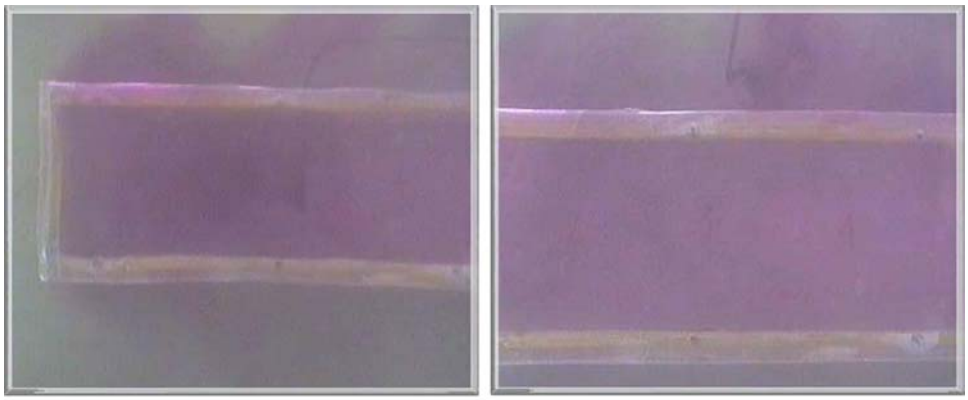

Figure 8 Flow visualisation at the fourth window on right side (winr4): (a) injection inside the model and (b) injection at the window plane (see online version for colours)

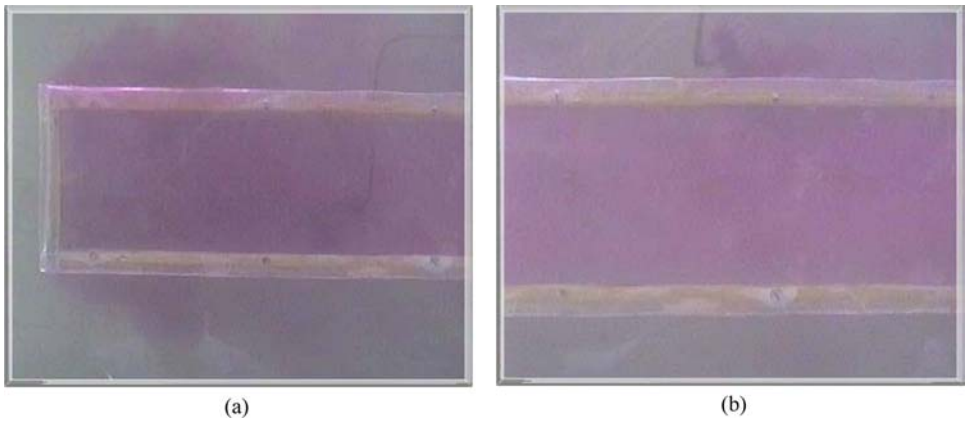

Figure 9(a) shows that the dye injected inside at winr5 mixes intensely, moves towards the front face and exits from the windows ahead of winr5 on both sides, while a small amount diffuses downstream. Figure 9(b) shows that at the window face, there is a strong inflow.

Figure 10(a) shows that at the 6th window on the right (winr6), the dye moves towards the front and a small fraction moves to the rear. The forward flow exits primarily through winr1, winr2, winr3, winl1 and winl2, while a small portion exits through winr4 and winl3. Dye injected at the window face (Figure 10(b)) moves into the interior and disperses vigorously. At the second last window (winr7), Figure 11(a), the dye mixes vigorously, moves towards the front and exits through first four windows on right side and first three windows on left side. There is no outflow through the middle windows. In Figure 11(b), flow through the window plane is inwards and a small amount flows along the exterior towards the rear. At the last window on right (winr8), Figure 12(a), there is intense mixing

accompanied by flow towards the front that exits through the front windows (winr1–winr4, winl1–winl3). At the window plane, there is a weak inflow while a small amount flows towards the rear face (Figure 12(b)). Internal flows at winr7 and winr8 are strongly three-dimensional and turbulent.

Figure 9 Flow visualisation at the fifth window on right side (winr5): (a) injection inside the model and (b) injection at the window plane (see online version for colours)

(a) (b)

Figure 10 Flow visualisation at the sixth window on right side (winr6): (a) injection inside the model and (b) injection at the window plane (see online version for colours)

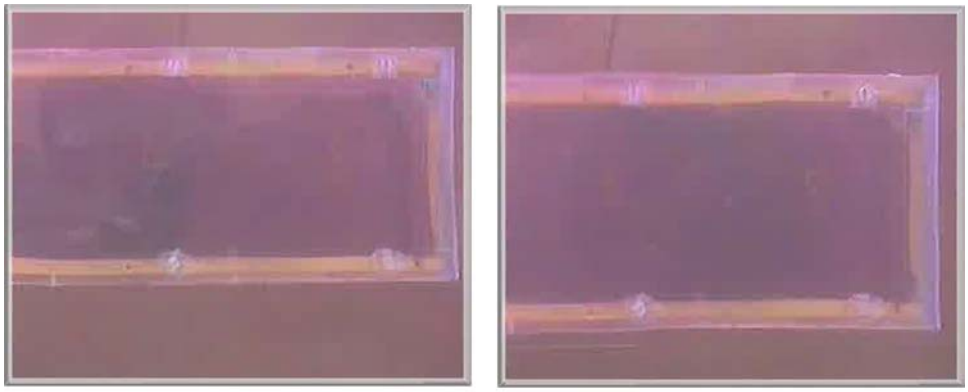

(a) (b)

4.2 Flow over the roof

In Figure 13, the dye is injected at the front face and the picture is taken from the side. In the vertical plane, the dye moves upwards to the roof and separates to form the recirculation region on the roof that extends up to approximately 2 W. It can also be seen that after reattachment there is small upward flow that moves downstream along the roof towards the bus rear. There is strong mixing between the fluid in the recirculation region and the free stream. Overall, this flow has the general features of separation-reattachment bubble over a bluff body, there is, though, additional inflow from front window outflows (Figures 5(a)–6(b)).

Figure 11 Flow visualisation at the seventh window on right side (winr7): (a) injection inside the model and (b) injection at the window plane (see online version for colours)

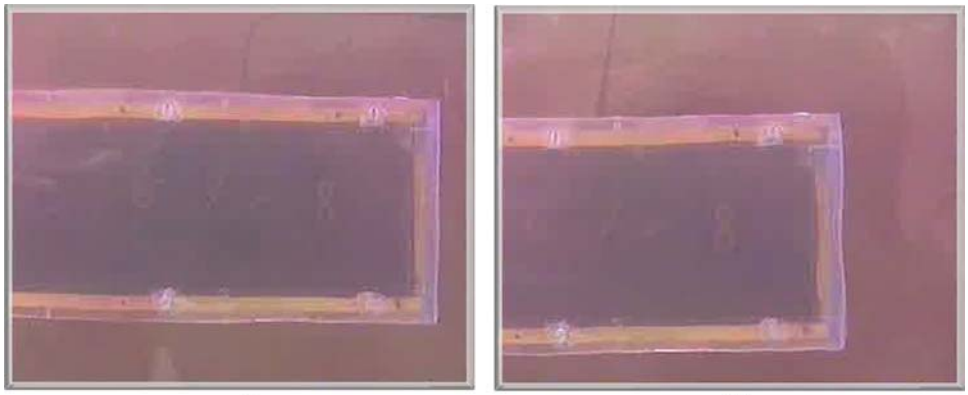

(a) (b)

Figure 12 Flow visualisation at the eight (last) window on right side (winr8): (a) injection inside the model and (b) injection at the window plane (see online version for colours)

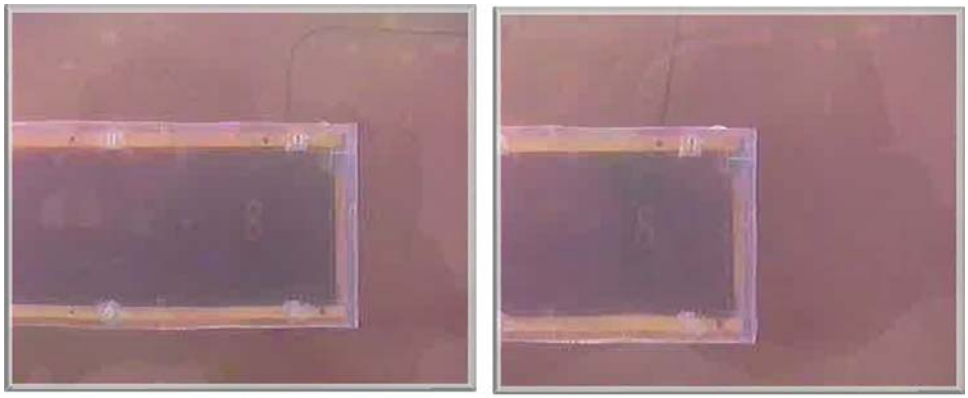

(a) (b)

Figure 13 Flow visualisation over the roof (see online version for colours)

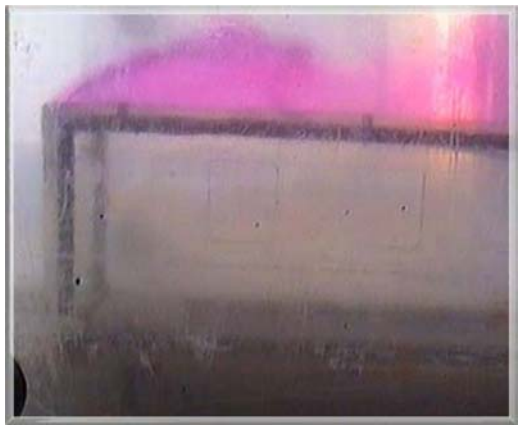

4.3 Wake flow

In Figure 14, the dye is injected at the centre of the rear face and this photo taken from above shows transverse mixing and a typical bluff body wake. It was observed that this flow was transitory with vertical symmetry at some instants and asymmetric flow most of the time. The wake extends to about 2.3 bus heights.

Figure 14 Flow visualisation in the wake (see online version for colours)

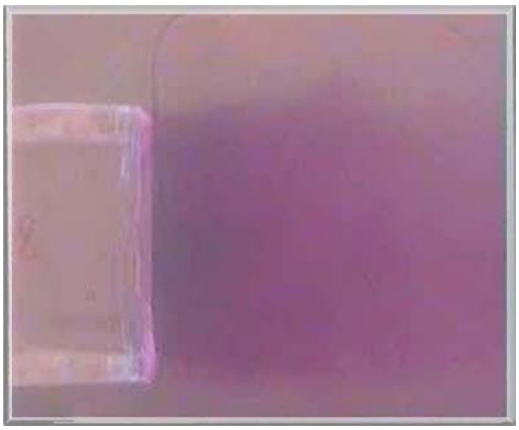

5 Numerical simulations for reference case (Case 1)

Vector plots from the numerical simulations at different planes are discussed here. The velocity magnitude was obtained by averaging over a period of 27.6 s.

5.1 Flow at the windows

Figures 15(a)–(h) show the velocity vector plots in a y–z plane (transverse) passing through the vertical centre line of the window. The view is looking towards the bus front from rear, i.e., free-stream flow is out of the paper.

At the first window, winr1, Figure 15(a), air exits with velocities of 2–5 m/s. Air exiting from the top portion of the window moves along the side wall into the recirculation region on the roof of the bus. The air exiting through the bottom portion of the window moves down along the sidewall and mixes with the free-stream. In Figure 15(b), the y–z plane cuts across winr2 and winl1 as they are opposite one another. Air exits both windows with comparable velocities of 4 m/s. The transverse spread relative to winr1 is more at winr2. Due to the asymmetry of the flow, the spread at winr2 is also larger than that at winl1 although they are centred at the same axial location. Here, too, some air moves upwards and is captured in the recirculation zone over the roof.

In Figure 15(c), the plane cuts windows winr3 and winl2. At both windows, air exits from the bus and the lateral spread is more than that at winr2. The spread is asymmetric being larger on the right side. Distinct eddies are seen above and below the window exterior and the former carries air to the recirculation zone over the roof.

Figure 15(d) shows that at winr4 and winl3, the air flows outwards however, velocities are low, about 1 m/s. The outflow from the opposite window, winl3, moves upwards but unlike the flow exiting from the front windows, it does not move to the recirculation zone over the roof. From the top of the left window some air moves inside the bus. The lateral spread and recirculation zone height are about 0.5 W.

The inflow through winr5 and winl4 is seen in Figure 15(e). From the latter it enters at high velocities (3–7 m/s) whereas through winr5 it is much lower (<1 m/s).

Figure 15(a) Vector plot at a vertical transverse plane across the first window on right (winr1)

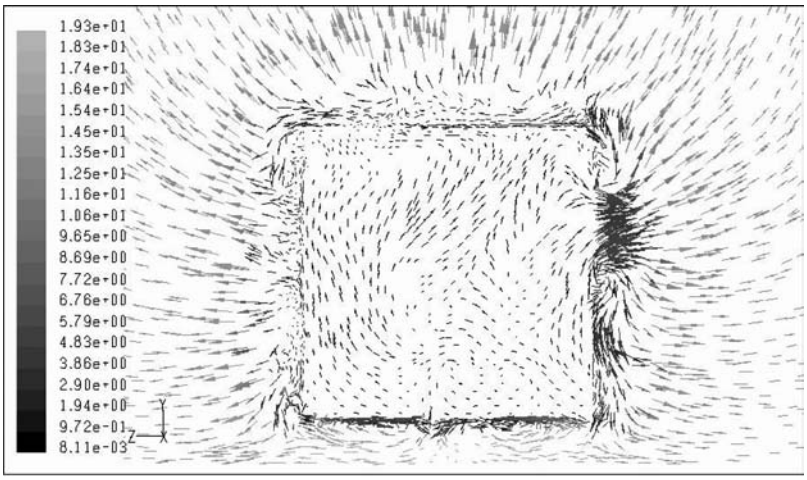

(a)

Figure 15(b) Vector plot at a vertical transverse plane across the second window on right (winr2). Opposite window winl1 is also seen

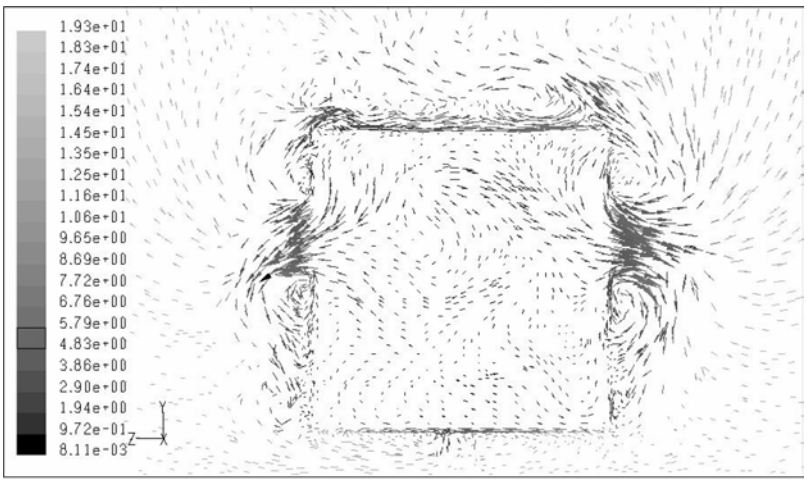

(b)

At windows winr6 and winl5, Figure 15(f), air enters through both windows at high velocities (4–8 m/s). Some of the air flows from the roof along the walls and into the windows. Figure 15(g) shows air entering through winr7 with high velocity (4–8 m/s); on the left side the door is closed. Some of the air entering the bus comes from the roof. At the rearmost windows, winr8 and winl7, air enters at high velocities (6–9 m/s), Figure 15(h). Down-flow from the roof into the windows is clearly seen, especially on the right.

Figure 15(c) Vector plot at a vertical transverse plane across the third window on right (winr3). Opposite window winl2 is also seen

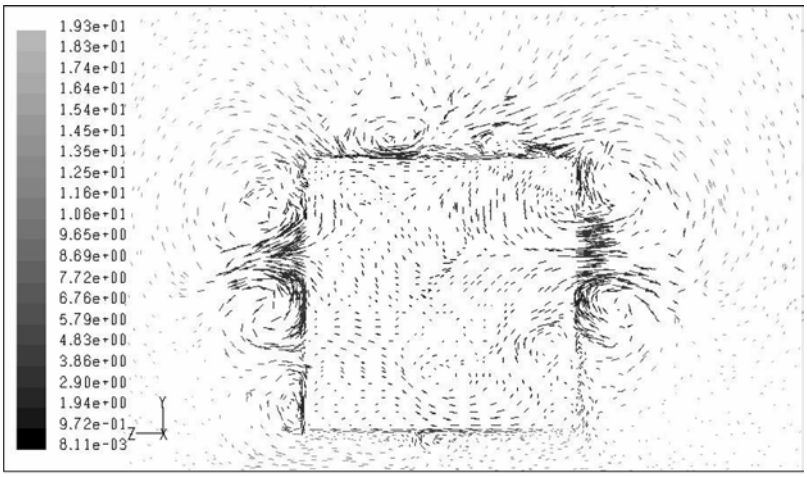

(c)

Figure 15(d) Vector plot at a vertical transverse plane across the fourth window on right (winr4). The opposite window winl3 is also seen

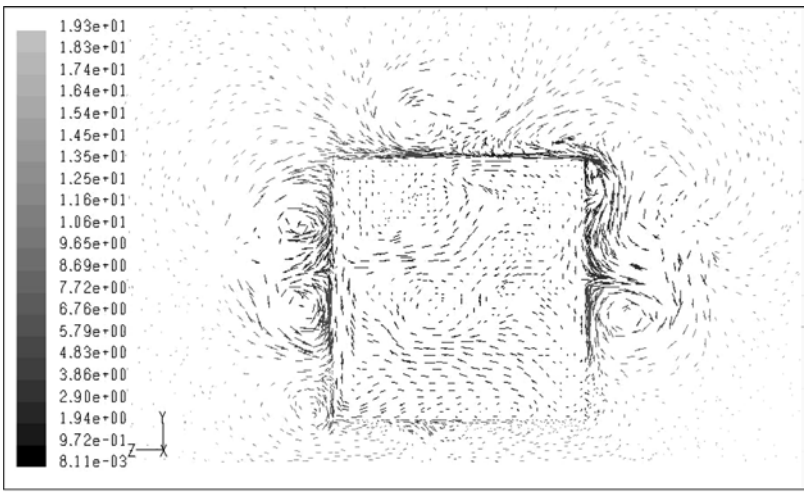

(d)

Figure 15(e) Vector plot at a vertical transverse plane across the fifth window on right (winr5). The opposite window winl4 is also seen

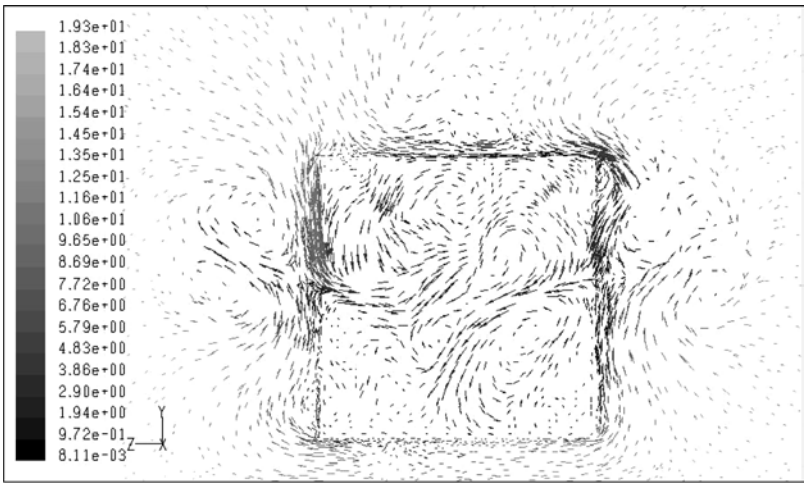

(e)

Figure 15(f) Vector plot at a vertical transverse plane across the sixth window on right (winr6). The opposite window winl5 is also seen

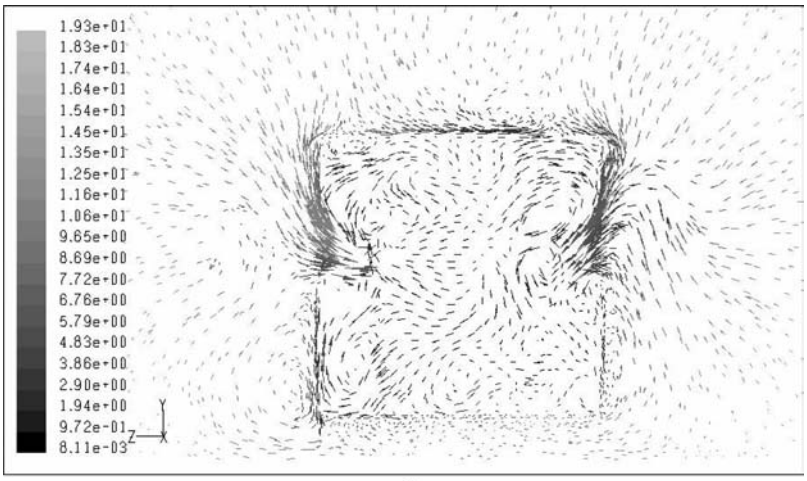

(f)

The consolidated picture that emerges from these plots is that on the right side air exits through the first four windows, at the fifth window there is a weak outflow while at the rear three windows there is inflow. On the left side, air exits through the first three windows, through the fourth window there is no clear trend (i.e., through 1/4th of the window there is inflow whereas through the remaining part there is outflow), and through the two rear windows there is an inflow.

Figure 15(g) Vector plot at a vertical transverse plane across the seventh window on right (winr7)

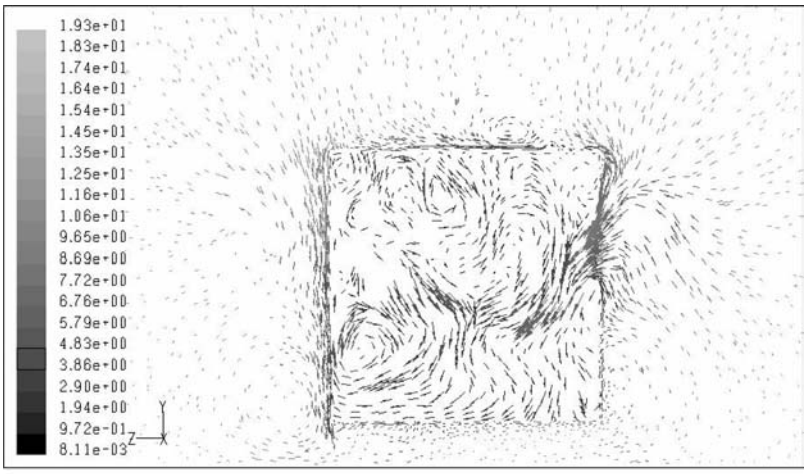

(g)

Figure 15(h) Vector plot at a vertical transverse plane across the eighth window on right (winr8). The opposite window winl6 is also seen

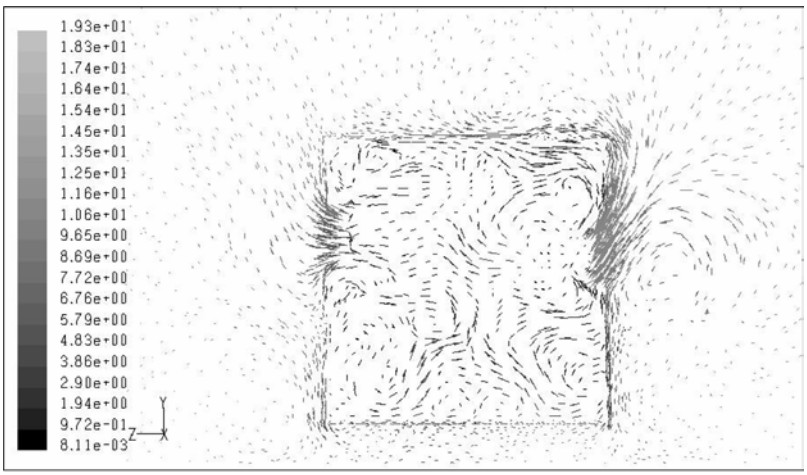

(h)

5.2 Flow in vertical longitudinal $(x - y)$ planes

Figure 16(a) shows the vector plots in a vertical, longitudinal $(x - y)$ plane through the bus centre. The recirculation region on the roof extends up to approximately 2 W. The wake consists of a pair of large structures that are stretched downstream up to approximately 3 W. A small region of accelerated flow between the ground and the vehicle floor is also seen. The inside flow is dominated by air moving from rear to the front, except for a small portion at the rear where it moves downstream. There are two distinct regions, one, a black region in the upper portion with

negligible velocities that occupies almost 50% of the area and, second, a dark grey region in the lower half of the bus where velocities are up to 0.9 m/s that occupies the remaining half. In general, inside velocities are low.

Figure 16(a) Vector plot at a vertical longitudinal plane through bus centre

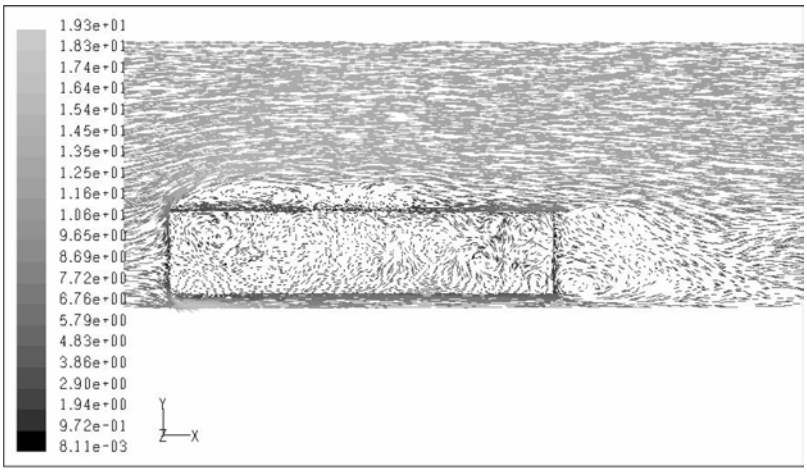

(a)

Figure 16(b) Vector plot at a vertical longitudinal plane inside the bus and offset by 0.1 m from the right side

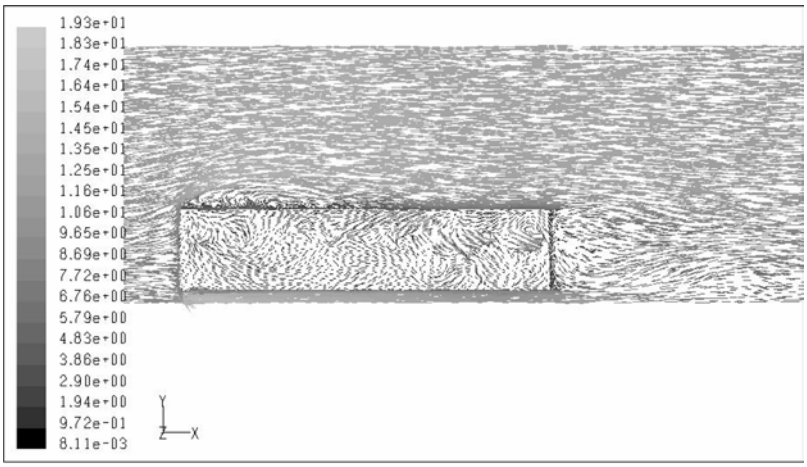

(b)

Figure 16(b) shows vector plots in a vertical longitudinal plane that is adjacent to the right wall at a distance of 0.1 m from it. Four regions can be distinctly seen. The black region which covers some of the top portion from front half and a portion from the rear constitutes 20% of the area and has negligible velocities. The dark grey region occupies 50% of the area covers most of the front half of the bus and has low velocities (<0.9 m/s). The grey area that covers 20% of the area

Figure 16(c) Vector plot at a vertical longitudinal plane inside the bus and offset by 0.1 m from the left side

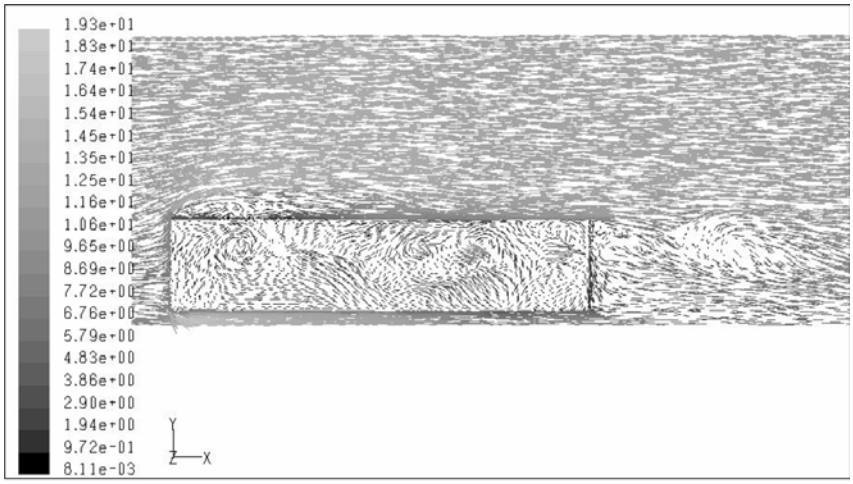

(c)

occupies a space between winr3 and winr8 in the vicinity of the roof and the floor of the bus; here velocities are between 0.9 m/s and 1.9 m/s. These velocity magnitudes are desirable from comfort standpoint but they exist away from the breathing zone (1.45 m above bus floor). Finally, the light grey area covers 10% of the area and extends from winr5 to winr8 and is close to the windows. Here, velocities are high between 2 m/s and 6 m/s which are high from comfort standpoint.

Figure 16(c) shows vector plots in a vertical longitudinal plane inside the bus just adjacent to left side and displaced by 0.1 m. The flow field is similar to that discussed above at the plane near the right side. The only difference is that the grey region (0.9–2 m/s) has increased by 5% at the expense of the dark grey area ($<$0.9 m/s).

5.3 Flow in horizontal longitudinal $(x - z)$ plane

Figure 17 shows the vector plots in a horizontal $(x - z)$ plane that is 1.85 m above the road surface or 1.45 m above the bus floor. This is the plane where passengers would be breathing. Due to the presence of the windows, the recirculation zones on the sides of the bus extend much further than that on the roof. On the right side it extends up to end of the bus while on the left it extends up to the rear door (which is closed). Also, the spread of recirculation zone in the lateral direction is more on the right. The velocities with which air enters the bus from the rear windows is almost twice at with which it exits through the front windows. Since mixing is turbulent, this circulation from front to rear windows outside the bus causes mixing with the free stream resulting in replenishment of fresh air in the bus.

Three distinct regions can be identified. The largest area, 70% of total, is black and it occupies the central region away from the windows, here, the velocities are negligible. The grey colour covers 15% of the area, near the walls and the mixing

zone between light grey and black region, here the velocities are up to 0.9 m/s. The remaining 15% of the area is close to the rear windows and has high velocities, 4–8 m/s. The wake extends to approximately 3 W and has two counter rotating eddies attached to the rear and another large eddy near the ground.

Figure 17 Vector plot at a horizontal plane 1.45 m above the bus floor (1.85 m above domain floor)

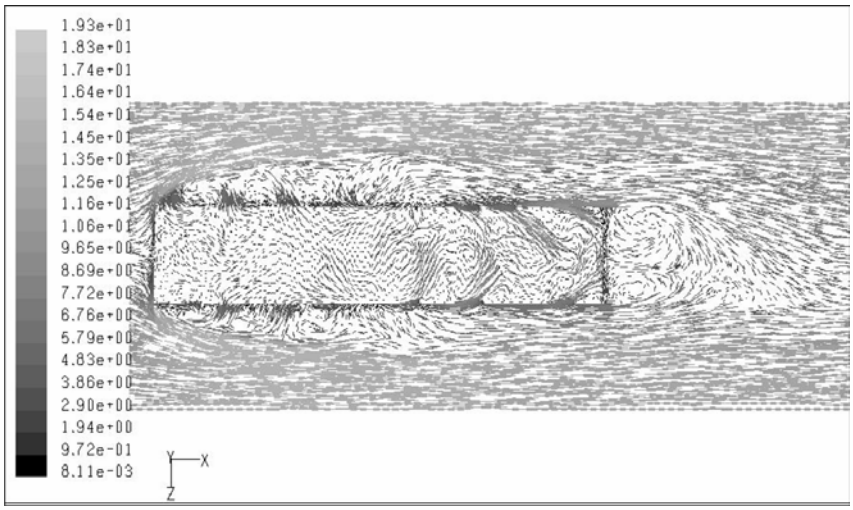

In summary, from Figures 16(a) and (b), the structure of the recirculation region on the roof as well as the wake are asymmetric which can be attributed to asymmetric window placements and strong three-dimensionality of the through flow that connects external and internal flows. Also, ventilation inside the bus is localised to a small region with substantial variations across the length and breadth. As a consequence of the low velocities inside the bus passenger comfort is likely to be inadequate. This section and the previous one establish that for the reference case, flow features from visualisation and numerical simulations are in good agreement. Thus, the numerical model constants are reasonably tuned.

6 Design interventions

From the above, it is clear that there are substantial regions inside the bus with very low air velocities and there is a need to decrease this space. It is, therefore, necessary to induce additional airflow through the bus for which strategic openings on the body would be required; henceforth, such openings are referred to as interventions. A possible reduction in the drag would be an added advantage. Based on practical considerations, seven candidate interventions were identified. These are:

- one horizontal slot on the front above the windshield (slot_front, size 2.25×0.375 m, centroid 2.16 m above floor)

- three slots on the roof, viz., slot_top1 on roof front (0.45×0.45 m, centroid 1.78 m from front), slot_top2 on roof middle (0.45×0.45 m, centroid 4.78 m from front), and slot_top3 at the rear portion of the roof (1×1 m, centroid 7.77 m from front)
- three horizontal slots (2.25×0.375 m) at the rear, viz., slot_rear1 at the upper part, slot_rear2 at the middle and slot-rear3 at the bottom with respective centroids located 2.16, 1.25 and 0.34 m above the floor.

The size and location of interventions were selected from the flow field knowledge of the reference case.

By selectively opening and closing these interventions, seven different designs of the bus body were generated and designated as Cases 2–8; details are given in Table 2. Visualisation experiments were performed by replacing appropriate panels on the brass frame for Cases 1, 2 and 6. For comparison, a simulation was also performed with all windows closed in the reference case, designated Case 0.

Table 2 Arrangement of interventions

Intervention	*Case 1*	*Case 2*	*Case 3*	*Case 4*	*Case 5*	*Case 6*	*Case 7*	*Case 8*
winr1	✓	✓	✓	✓	✓	×	×	✓
winr2	✓	✓	✓	✓	✓	×	×	✓
winr3	✓	✓	✓	✓	✓	×	×	✓
winr4	✓	✓	✓	✓	✓	✓	×	✓
winr5	✓	✓	✓	✓	✓	✓	×	✓
winr6	✓	✓	✓	✓	✓	✓	×	✓
winr7	✓	✓	✓	✓	✓	✓	×	✓
winr8	✓	✓	✓	✓	✓	✓	×	✓
winl1	✓	✓	✓	✓	✓	×	×	✓
winl2	✓	✓	✓	✓	✓	×	×	✓
winl3	✓	✓	✓	✓	✓	✓	×	✓
winl4	✓	✓	✓	✓	✓	✓	×	✓
winl5	✓	✓	✓	✓	✓	✓	×	✓
winl6	✓	✓	✓	✓	✓	✓	×	✓
slot_front	×	✓	✓	✓	✓	✓	✓	✓
slot_top1	×	✓	×	×	×	×	×	×
slot_top2	×	✓	✓	✓	✓	✓	✓	✓*
slot_top3	×	✓	✓	✓	✓	✓	✓	✓
slot_rear1	×	✓	✓	✓	×	✓	✓	✓+
slot_rear2	×	✓	✓	✓	✓	✓	✓	✓+
slot_rear3	×	✓	✓	×	✓	×	✓	×

Nomenclature:
✓ Intervention open.
× Intervention closed.
* Size increased.
+ Slot_rear2 and 3 merged by removing the space between them.

7 Effect of interventions on flow: visualisations

In the cases visualised (Cases 2 and 6), the flow at each of the interventions was qualitatively similar, the variations were in magnitude but these, too, were not very significant. In the discussion below, typical flow features are presented.

7.1 Flow at top slot on the front face (slot_front)

In Figure 18(a) (Case 2), the dye is injected just upstream of the front slot and picture is taken from the top. It enters the bus at a high velocity and does not diffuse up to 0.3 W, i.e., the stream remains almost parallel up to this point, and then diffuses downstream all the way to the rear. Figure 18(b) shows the same flow for Case 3 where the front slot on the roof (slot_top1) is closed. Compared to the other case depicted in Figure 18(a), the flow stream remains parallel inside the bus for a longer distance, i.e., 0.8 W.

Figure 18 Flow visualisation at the interventions: (a) injection at the front slot (slot_front) face; (b) injection downstream of the front slot (slot_front) inside the model; (c) injection at the front slot on the root (slot_top1); (d) injection at the middle slot on the roof (slot_top2); (e) injection at the rear slot on the root (slot_top3); (f) injection at the upper rear slot (slot_rear1); (g) injection at the middle rear slot (slot_rear2); (h) injection at the bottom rear slot (slot_rear3) (see online version for colours)

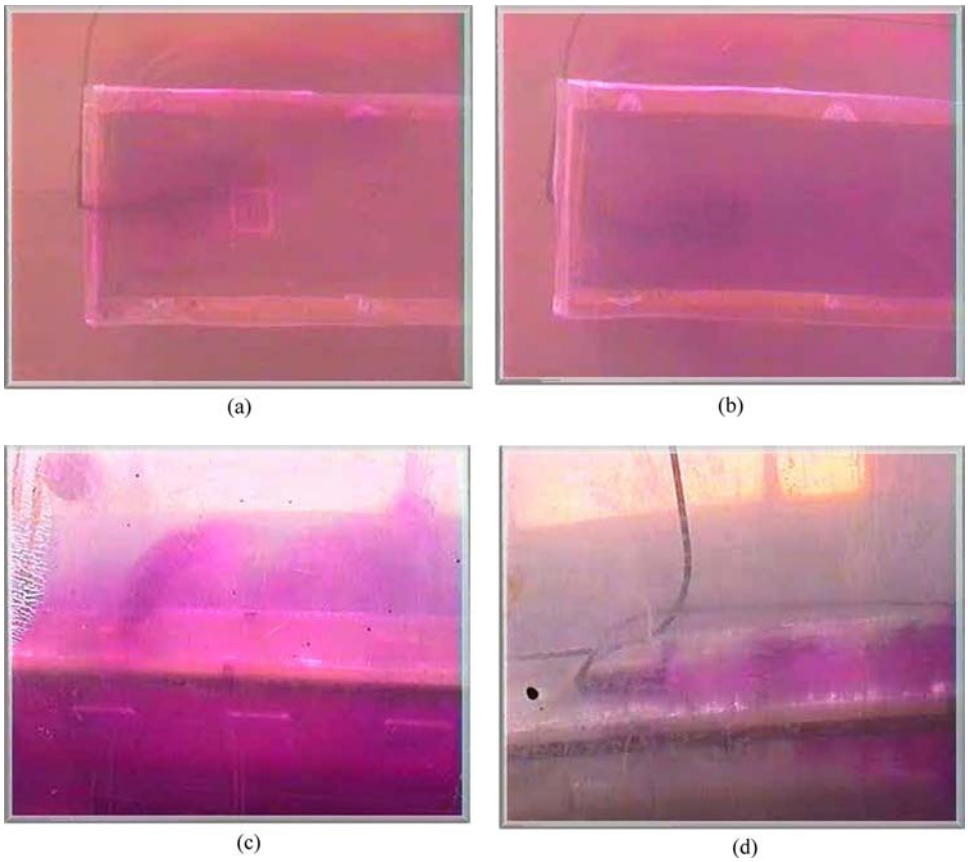

Figure 18 Flow visualisation at the interventions: (a) injection at the front slot (slot_front) face; (b) injection downstream of the front slot (slot_front) inside the model; (c) injection at the front slot on the root (slot_top1); (d) injection at the middle slot on the roof (slot_top2); (e) injection at the rear slot on the root (slot_top3); (f) injection at the upper rear slot (slot_rear1); (g) injection at the middle rear slot (slot_rear2); (h) injection at the bottom rear slot (slot_rear3) (see online version for colours) (continued)

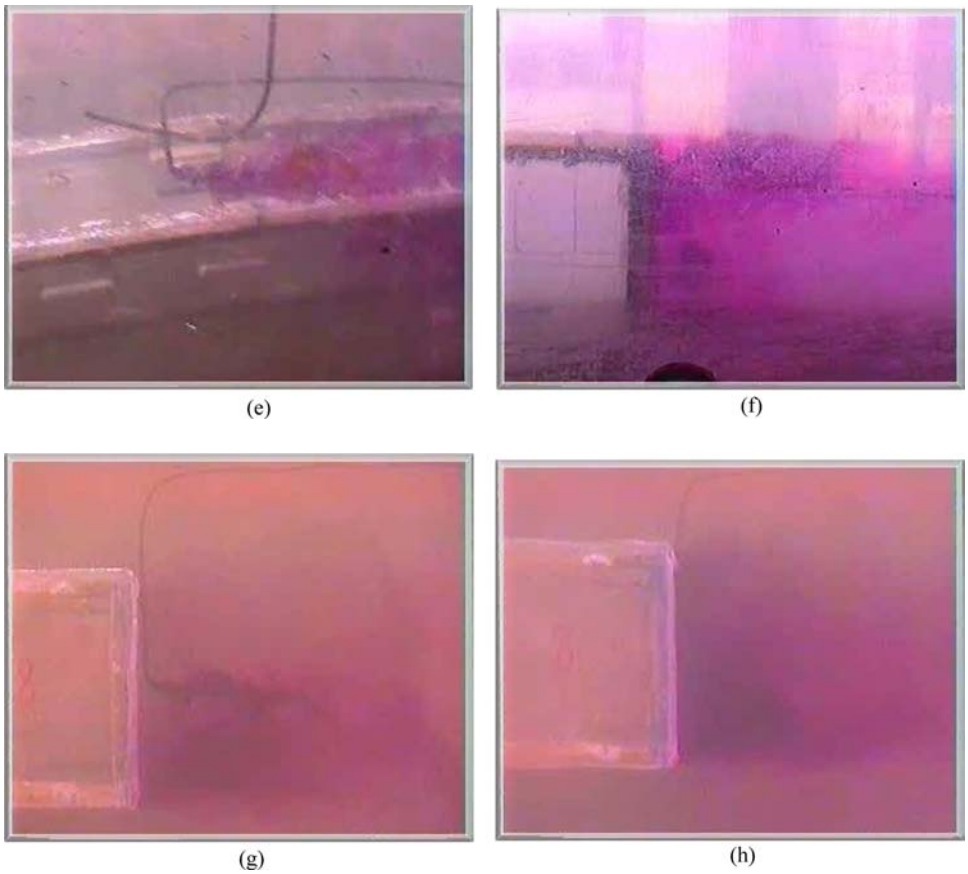

7.2 Flow at the roof slots

Figure 18(c) is an oblique view from the top and dye injection in the interior. There is outflow thorough the front slot (slot_top1) into the recirculation region over the roof, consequently, the reattachment length increases. The outflow velocity is high. In Figure 18(d) dye injected just above the face of the middle roof slot flows inwards. In Figure 18(e), the dye is injected on the roof top just ahead of the rear roof slot (slot_top3) and it flows inwards.

7.3 Flow at the rear slots

Figure 18(f) shows that dye injected just downstream of the upper slot on the rear face is carried away into the wake at a high velocity, disturbs the wake and diffuses

further downstream. This slot facilitates movement from interior into the wake that is very desirable. At the middle slot on the rear also, a similar pattern is visible, i.e., high velocity outflow into the wake, Figure 18(g). The length of wake in the longitudinal direction is increased but unlike Case 1, it is now split into two or three parts and has become wavy. In Figure 18(h), the dye was injected just downstream of the bottom slot on the rear face. The dye exits at low velocity and spreads laterally along the back side. Thus, this slot is not very effective in augmenting outflow.

8 Effect of interventions on flow: simulations

Numerical simulations of the effects of interventions are discussed for Case 8 which as described in the next section is the best combination for comfort enhancement and drag reduction. The geometry of this case is shown in Figure 19 and includes a front slot, roof slots at middle and rear (each $1\,\mathrm{m} \times 1\,\mathrm{m}$), and a slot on upper half of the rear (by combining upper and middle slots). The broad features are as described earlier and unique aspects are described below.

Figure 19 Interventions for Case 8

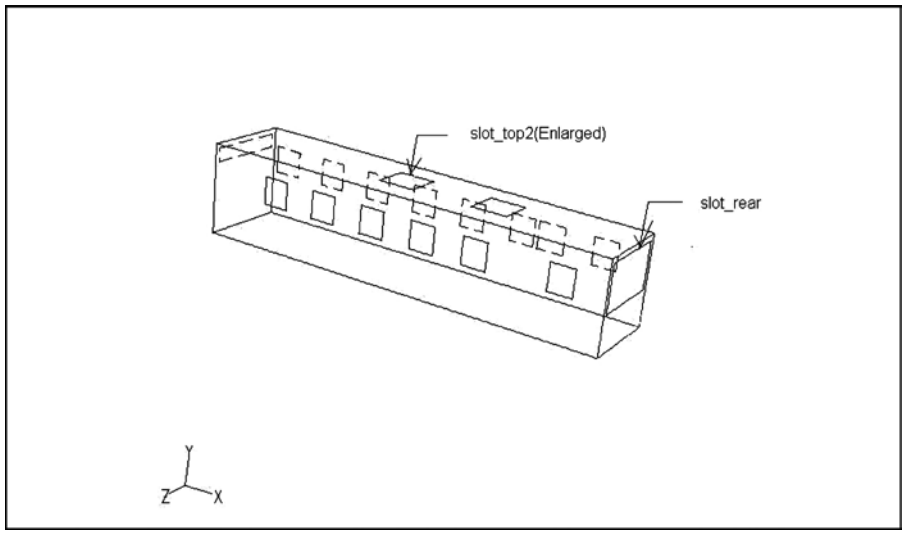

Figure 20(a) shows velocity vectors at the longitudinal centre plane. Oncoming air flows below the bus, through the front slot and above the roof. Incoming air from the front slot continues up to middle roof opening. There is outflow through the rear slot that has strongly altered the wake and the typical wake of a bluff body is seen only at the bottom portion. Inflow occurs at both the roof openings. Regions of negligible velocity ($<0.02\,\mathrm{m/s}$) cover 10% of the area (black region) and these are randomly distributed. The dark grey colour represents velocities less than $0.9\,\mathrm{m/s}$ and these occupy 20% of the area mostly at front half and near the rear face. The grey colour represents velocities between $0.9\,\mathrm{m/s}$ and $1.8\,\mathrm{m/s}$ and it occupies 40% of the area; this represents the comfort zone. Another 20% area (light grey)

has velocities between 1.8 m/s and 2.8 m/s while the remaining 10% (faint grey) has very high velocities (>2.8 m/s), which is not desirable from comfort viewpoint. High velocities are encountered at the inlet of the roof slots and such regions could be modified by suitable ducting for distributing it internally as well as reducing the velocity. The reattachment at the top occurs at approximately 2 W and the height of recirculation zone is 0.3 W. The air exits through the rear slot with high velocities, 4–5 m/s, breaks the wake which becomes wavy with high velocities in contrast to Case 1.

Figure 20 (a) Vector plot at a vertical longitudinal plane through the bus centre and (b) vector plot at a horizontal plane 1.45 m above the bus floor (1.85 m above domain floor)

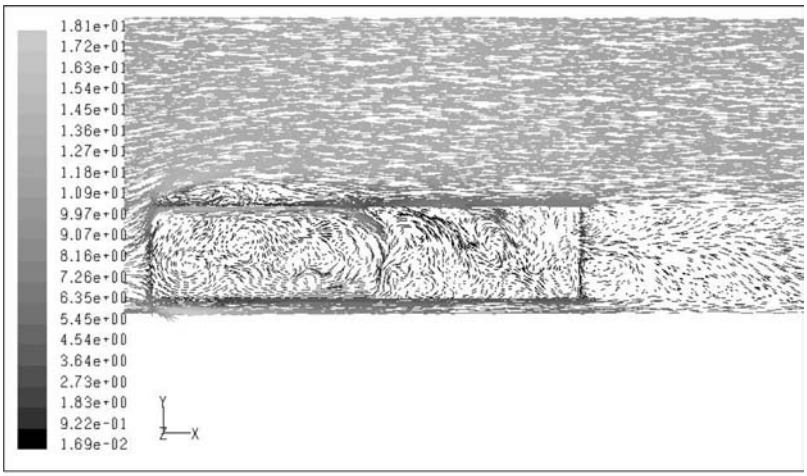

(a)

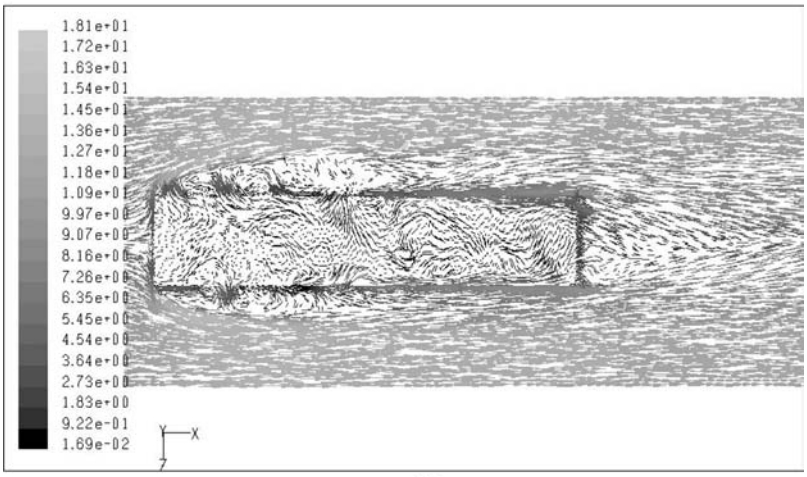

(b)

Figure 20(b) shows velocity vectors at a horizontal plane 1.85 m above the road surface (1.45 m above bus floor). The oncoming flow separates on the sides to form

separation bubbles however, due to asymmetry of the windows the bubble on the right is longer and wider than on the left. Outflow through the rear slot is also clearly seen. It can be seen that 20% of the area distributed randomly has negligible velocities (black colour) and another 20% has velocities up to 0.9 m/s (dark grey) that occupies most of the front half away from windows. About 35% of the area in grey has velocities of 0.9–1.8 m/s in the region near the windows and some portion in the rear half. Another 15% of the area has velocities of 2.8–4 m/s (light grey) and occupies a region in the rear half. The balance 10% of the area (in faint grey colour) has high velocities that are greater than 4 m/s and occupies the area in the middle portion. The flow through the rear slot is unidirectional and two weak recirculation regions are seen above and below.

The net effect of the interventions has produced considerable improvement in the through flow. Unlike Case 1, in the rear portion and top half the flow enters from the slots (except those on the rear) moves all the way inside the bus from front to rear and exits from the rear slots.

9 Effects of interventions on drag and through flow

As mentioned earlier, Cases 2–8 are variants of the reference case, Case 1. A summary of the effects interventions for each case is given in Table 3 and it includes drag force, through flow rates and comfort zone fraction. The through flow refers to the total inflow through all openings (which matches with the total outflow through all openings within 0.1%). Table 3 summarises the results for all the nine cases studied; in the table Case 1 has been taken as the reference and all changes are reported relative to Case 1. In the discussion below we have focused on the drag force and through flow. The lateral force was negligible in all cases as expected and the maximum value was less than 6% of the drag force. All the nine cases showed a downward force whose magnitude varied from 30 to 50% of the drag force.

With the objective of increasing through flow, all the slots (Figure 3) were opened (Table 2) that resulted in Case 2 configuration. As a result, the drag changed from 607 N in Case 1 to 514 N, a decrease of 15%. Simultaneously, the through flow increased from 10.4 m/s to 17.2 m/s, an increase of 65% (Table 3). While both these trends are desirable, the magnitude of change, however, was less than expected. The implication is that these interventions need to be further tuned.

Case 3 is a variant of Case 2 with the roof front slot closed. Relative to Case 2, there was almost no change in the drag, however, the through flow decreased by about 7.5%. Air flowing out from the roof front slot increased the size of the recirculation region on the roof and increased the reattachment length. Both these are undesirable effects and it was decided that the first slot on the bus roof be kept closed. This change was effected on all subsequent cases (Cases 4–8).

The effect of rear slots was next investigated. Two modifications of Case 2, one with rear bottom slot closed (upper and middle slots open) and the other with the rear upper slot closed (middle and bottom slots open) resulted in Cases 4 and 5, respectively. In Case 4, the drag is 15% less in comparison to Case 2 but the through flow has decreased by 9%. This drag reduction is significant even though it is realised at the expense of through flow. In Case 5, the drag is 9% less than Case 2 but 6% more than Case 4. The through flow is 12% less than Case 2 and

2% less than Case 4. These two sets of interventions indicate that keeping the rear upper slot open is more advantageous than opening the bottom slot.

Table 3 Drag and efflux values for all cases

Case no.	*Force (N) (Numbers in brackets indicate change w.r.t Case 1)*			*Through flow* (kg/s)
	Longitudinal (Drag)	*Vertical (Lift)*	*Lateral (Side)*	
Case 0	582 (−4.1%)	−187 (−14.2%)	−33 (+371.4%)	0
Case 1	607 (0.0%)	−218 (0.0%)	−7 (0.0%)	10.4 (0.0%)
Case 2	514 (−15.3%)	−176 (−18.8%)	1 (−83.9%)	17.2 (+65.0%)
Case 3	513 (−15.5%)	−174 (−19.9%)	9 (+22.9%)	16.7 (+60.3%)
Case 4	438 (−27.9%)	−185 (−15.05%)	27 (+284.3%)	15.7 (+50.1%)
Case 5	466 (−23.2%)	−213.8 (−01.8%)	6 (−19.7%)	15.4 (+47.4%)
Case 6	519 (−14.5%)	−160 (−26.5%)	−4 (−41.7%)	9 (−14.6%)
Case 7	474 (−21.9%)	−130 (−40.3%)	10 (+43.2%)	8 (−24.8%)
Case 8	431 (−28.9%)	−217 (−0.2%)	27 (+283.9%)	17 (+65.8%)

In Case 6, all windows in the bus front, i.e., winr1, winr2 and winr3 on right side and winl1 and winl2 on the left side were closed. The front slot on the roof and the bottom slot at the rear were also closed. This modification to Case 4 caused a 18% increase in drag and a 43% decrease in through flow. Clearly, the objective to have the air exit from the rear windows and the rear slots is not realised. Case 7 is an extreme version of Case 6 with all windows closed. The first slot on the roof was closed and all slots at the rear were kept open. Compared to Case 4, the drag increased by 8% and through flow decreased by 50%. Thus, Case 7 is also not desirable.

From the above discussion, Case 4 gives the best improvements as a result of the interventions. Finally, two modifications were done to Case 4 to produce Case 8, viz.,

- the size of the middle roof slot was increased from 450×450 mm to 1000×1000 mm
- the separator between the upper and middle slots at the rear was removed to produce a large slot that at the upper half on the rear.

The effects of these interventions as compared to Case 4 were a 1.6% drag reduction and 8% more through flow. Clearly, larger slots on the roof and rear (upper half) have a very favourable effect on through flow without much impact on drag.

Table 4 shows a detailed comparison between the existing bus (Case 1) and our best configuration (Case 8). Clearly, the comfort zone is considerably increased in Case 8 as discussed earlier.

Table 4 Comparison of comfort level in Cases 1 and 8

	Percentage of interior region occupied in breathing zone	
Order of velocity (m/s)	*Case 1 existing configuration*	*Case 8 proposed configuration*
Negligible (less than 0.1)	70	20
Low (0.1–0.9)	15	20
Significant (0.9–4.0)	11	52
Very high (more than 4.0)	4	8

In summary, the best interventions are those in Case 8 followed by those in Case 4. Overall, compared to the base case (Case 1), Cases 8 and 4 give drag reductions of 29 and 28%, while augmenting through flow by 66 and 50%, respectively. Keeping the roof front slot closed also ensures that the rear roof slots bring in fresh air. One large opening spanning the upper half of the bus rear may not be feasible and a more attractive option would be a series of smaller horizontal slots. On dusty roads, this arrangement could pose an additional problem in that when the vehicle slows to a stop, the entrained dust in the wake enters the passenger cabin from the rear openings. This aspect can be addressed by installing swinging louvers or similar mechanisms that would remain closed below a certain speed, say 10 km/h and open at higher speeds.

For completeness of discussion, the drag of the reference case, Case 1, was compared with the case where all windows and openings are closed; this case is designated as Case 0. The drag with open and closed windows was 607 N and 582 N, respectively, in other words, the open windows result in a 4% increase in drag. The closed window vehicle has no fresh air coming into the interior.

These investigations indicate that, interventions on open window, non-air conditioned buses can simultaneously enhance fuel economy via drag reduction, as well as passenger comfort. In most countries, intra-city (i.e., urban) buses as well as inter-city buses cater to the bulk of the passenger trips. On per passenger per kilometre basis, buses are significantly less polluting and more energy efficient than automobiles and two-wheelers. In tropical climates, the augmentation in ventilation as a result of interventions recommended here will provide a cost-effective as well as eco-friendly method of making bus-based transport more comfortable. Such buses could go a long way to promoting sustainable transport as against the alternative of higher cost and energy intensive option of closing all windows and air conditioning the bus.

10 Conclusions

The visualisations and numerical simulations on the open window bus have shown that there are major differences from the well-studied closed vehicle with a smooth exterior. The combination of open windows, an open front slot, open slots on

the roof at middle and rear, and open slots on the rear side at top and middle, result in the significant drag reduction (up to 29%) and, simultaneously enhance through flow (up to 65%). These interventions can provide a low-cost eco-friendly solution for enhancing passenger comfort vis-à-vis air conditioning the bus which is costly and energy intensive.

Acknowledgements

This work was partially supported by Volvo Research and Educational Foundations.

References

Duell, E.G. and George, A.R. (1999) *Experimental Study of a Ground Vehicle Body Unsteady Near Wake*, SAE Paper 1999-01-0812.

Fluent (2003) *Fluent® 6.1, User's Guide. 10. Modeling Turbulence, 10.7, The Large-Eddy Simulation Model*, Fluent Inc.

Kim, M-H. (2004) 'Numerical study on the wake flow characteristics and drag reduction of large-sized bus using rear spoiler', *Int. J. Vehicle Design*, Vol. 34, No. 3, pp.203–217.

Krajnovic, S. and Davidson, L. (2002) 'Exploring the flow around a simplified bus with Large Eddy Simulation and topological tools', in McCallen, R., Browand, F. and Ross, J. (Eds.): *The Aerodynamics of Heavy Vehicles: Trucks, Buses and Trains*, Springer, Heidelberg, pp.49–64.

Mousley, P.D. and Watkins, S. (2000) *A Method of Flow Measurement about Full-Scale and Model-Scale Vehicles*, SAE Paper 2000-01-0871.

Roy, S. and Srinivasan, P. (2000) *External Flow Analysis of a Truck for Drag Reduction*, SAE Paper 2000-01-3500.

Sagaut, P. (2001) *Large Eddy Simulation for Incompressible Flows*, Springer, Germany.

Bibliography

Abdel Azim El-Safed, A.E. and Nassief, M.M. (1996) *Investigation into the Aerodynamics of the External Flow Around a Bus (Daewoo Model)*, SAE Special Publications, Vol. 1199, pp.59–68.

Basara, B. and Tibaut, P. (2002) *Time Dependent vs. Steady State Calculations of External Aerodynamics*, AVL List Gmbh, Graz, Austria, 8020.

Bradshaw, P. (1971) *An Introduction to Turbulence and Its Measurement*, Pergamon Press, Oxford.

McCallen, R., Browand, F. and Ross, J. (2002) *The Aerodynamics of Heavy Vehicles: Trucks, Buses and Trains*, Springer, Heidelberg.

Ota, D.K., Ramakrishnan, S.V., Szema, K-Y. and Chakravarthy, S.R. (1993) *Computation of External Automobile Body Shapes*, Rockwell International Science Center, D.F. Vitali, Centro Ricerche/DVC, FIAT. 932887, Italy.

Tennekes, H. and Lumley, J.L. (1972) *A First Course in Turbulence*, MIT Press, Cambridge, MA.

Nomenclature

C_{rng}	LES model constant
H	Height of bus
h	Height of water channel
$\bar{p}$	Mean pressure
Re	Reynolds number
t	Time
$\overline{u_i}$	Mean velocity in i direction
w	Width of water channel
W	Width of bus
x	Spatial variable
η	Kolmogorov length scale
μ	Dynamic viscosity
ρ	Density
τ_{ij}	Stress in j direction in a plane perpendicular to i axis